Supporting Information for

Hot carriers and photothermal effects of monolayer MoO_x for promoting sulfite oxidase mimetic activity

Yuan Chen, Xiaoju Wu, Tongming Chen and Guowei Yang*

State Key Laboratory of Optoelectronic Materials and Technologies, Nanotechnology Research Center, School of Materials Science & Engineering, Sun Yat-sen University, Guangzhou 510275, Guangdong, P. R. China.

* Corresponding authors: stsygw@mail.sysu.edu.cn

1. Chemicals and reagents

Ammonium molybdate tetrahydrate [$(NH_4)_6Mo_7O_{24}\cdot 4H_2O$, AMT], Glycine (Gly) were purchased from Shanghai Aladdin Reagent Co., Ltd. Potassium hexacyanoferrate (III) ($K_3[Fe(CN)_6]$) was offered by Shanghai Macklin Biochemical Co., Ltd. Sodium sulfite (Na_2SO_3) and Hydrochloric acid (37%) were obtained from Guangzhou Chemical Reagent Factory. Millipore water (18.2 MΩ) was used throughout the experiments.

2. Preparation of MoO_x nanoflowers

The MoO_x nanoflowers were synthesized according to the previous report initially set up by Wang and co-workers.[1] In a typical synthetic procedure, AMT (123.5 mg) was dissolved into Millipore water (20 mL) under vigorous stirring. Then Gly (0.35 g) was slowly added to obtain a homogeneous solution. After that, Hydrochloric acid (0.3 mL) was added dropwise under vigorous stirring for 6 h to adjust the pH of the above mixture. After mixing evenly, the mixture was transferred into a 50 mL Teflon-lined autoclave, and performed at 180 ºC for 10 h. Afterwards, the obtained dark blue precipitate was collected by centrifugation (10000 r.p.m., 5 min) and washed with deionized water. Finally, the products were obtained by freeze-drying and labeled as MoO_x NFs.

3. Preparation of monolayer-MoO_x aqueous solution

The monolayer-MoO_x was synthesized through dispersing the as-prepared MoO_x NFs in Millipore water, following by centrifugation measurement (4000 r.p.m., 5min). The collected supernatant fluid was labeled as ML-MoO_x aqueous solution.

4. Preparation of bulk MoO_3

The procedure of bulk MoO_3 was similar to that of the ML-MoO_x without the addition

of ethanol and Gly. And the obtained sample was labeled as b-MoO_3.

5. Apparatus and characterizations

The morphologies, quantitative and semi-quantitative element information of the as-prepared samples were characterized by a Field-Emission scanning electron microscopy (FESEM, Zeiss Gemini SEM 500) coupled with an energy dispersive X-ray spectroscope (EDS, Bruker X-flesh 5060f) and an FEI Tecnai G2 F30 transmission electron microscope (TEM). The thickness profile was observed by a Bruker Multimode 8 atomic force microscope (AFM). The X-ray diffraction (XRD) pattern was conducted on an X-ray diffractometer (D/Max-IIIA, Rigaku) at a voltage of 40 kV and a current of 20 mA at a scanning rate of 2º s^{-1}. The UV-vis-NIR spectra of the samples were performed by a spectrophotometer (UV-3600, SHIMADZU Corporation) with $BaSO_4$ as a reference. Fourier transform infrared (FTIR) spectra were carried out on an FTIR spectrometer (Frontier, PerkinElmer Company). Raman spectra were obtained by a Renishaw In Via Plus laser micro-Raman spectrometer using an argon ion laser (514.5 nm, 90 mW). X-ray photoelectron spectroscopy (XPS) were recorded on an X-ray photoelectron microprobe spectrometer (ESCLAB 250, Thermal-VF Scientific, Al Kα), all of the bindings to the C 1s peak of adventitious surface carbon at 284.8 eV. Thermalgravimetric analysis (TGA) was conducted to determine the composition and degree of reduction of MoO_x NFs. TG curves were recorded on a thermogravimetric analyzer (TG-209, Netzsch) from room temperature to 800 ºC at a heating rate of 10 ºC min^{-1} and a flow rate of 20 sccm in either air or nitrogen atmosphere. The degree of the reduction of the as-prepared samples could be estimated

from comparing the difference between the weight loss under air and nitrogen atmosphere. And the substoichiometry concentration x could be obtained from the balance Equation [2, 3]:

$$M_w\ (MoO_3) = (1 + [(\%\ \text{mass loss/gain in air}) - (\%\ \text{mass loss in } N_2)/100]) \times M_w(MoO_{3-x}) \quad \text{(S1)}$$

where M_w corresponds to the molecule weight.

The amount of Mo in ML-MoO_x was measured by inductive coupled plasma mass spectrometry (ICP-MS, Thermo Fisher). The specific surface areas were acquired by Brunauer-Emmett-Teller (BET) analysis via a Micromeritics ASAP 2020M system after vacuum degassing process at 120 ºC for 6 h. Electron spin resonance (ESR) solid powder analysis was performed on a Bruker EMX A300 spectrometer. All the ESR measurements were conducted under the room temperature at 9.86 Hz. ESR parameter settings were executed as follows: modulation amplitude 1 G, microwave power 2.20 mW and sweep time 40.96 ms. Electrochemical measurements were recorded on a CHI660E electrochemical workstation coupled with a three-electrode cell (a Pt sheet as the counter electrode, a saturated Ag/AgCl electrode as reference electrode) in Na_2SO_4 electrolyte (0.5 M, pH= 6.8).

6. Photothermal effect of ML-MoO_x aqueous solution

ML-MoO_x and b-MoO_3 aqueous solution with different concentrations were put into a glass beaker and irradiated by a laser (808 nm) at power densities of 100, 200, 300 mW cm^{-2}. Samples were illuminated from the top, and the thermographs were collected from

the side obtained via a thermal camera (Fluke Ti27). The incident light was turned off until reaching a steady state, and the temperature increment (ΔT) were obtained from the thermographs.

7. Dark-field scattering spectroscopy measurement

ML-MoO_x was deposited on microscope slides for *in-situ* observation. Before deposition, the microscope slides were immersed into acetone and sonication for 1 h to remove the surface dust impurities. Next, the slides were completely rinsed with Millipore water for removing the organic contaminants and endowing the slides with hydrophilicity. Then, one drop of the ML-MoO_x diluted solution which has been diluted for more than 20 times was transferred to a piece of clean pretreated slide. The loaded slides were finally dried with nitrogen gas. A dark-field scattering microscope (Olympus BX51) integrated with a quartz-tungsten-halogen lamp, a monochromator (Acton Spectra Pro, 2300i) and a charge-coupled device (CCD) camera (Princeton Instruments, Pixis 400BR_eXcelon) was conducted to collect the backward scattering spectra. The oblique incident white light was illuminated with a 53° incident angle on the samples. The scattering light was collected by a dark-field objective on top (LMPLFLN100XBD, numerical aperture=0.80).

8. Sulfite oxidase activity of ML-MoO_x

A colorimetric approach with $K_3[Fe(CN)_6]$ as an electron acceptor was performed to investigate the SuO_x activity of ML-MoO_x. Catalytic experiments were carried out through recording the reduction rate at 420 nm ($\varepsilon_{420\,nm} = 1.04\ mM^{-1}\ cm^{-1}$).[2, 4-7] The SuO_x activity was measured in a reaction volume of 600 μL Millipore water with $K_3[Fe(CN)_6]$

(0.15 mM) and different concentrations of ML-MoO_x (0-0.1 mg mL^{-1}). Immediately, Na_2SO_3 (0.3 mM) was added to start the reaction, prior to recording the absorbance on a UV 5200 PC spectrophotometer (Metash, Shanghai) for 150 seconds at room temperature. By contrast, the control experiments of b-MoO_3 were also conducted in similar constants. The enhanced sulfite oxidase-like activity of ML-MoO_x under light irradiation by a laser (808 nm) at different power densities was performed in a quartz cell (1.0*1.0*4.5 cm, 200 μL) in the presence of ML-MoO_x (0.05 mg mL^{-1}), K_3[Fe $(CN)_6$] (0.15 mM) and different concentrations of Na_2SO_3 (0-0.6 mM). The sulfite oxidase-like activity was monitored at 420 nm by real-time detection on a UV 5200 PC spectrophotometer (Metash, Shanghai) coupled with a thermocouple for 150 seconds[8].

Steady-state kinetic analysis of ML-MoO_x (0.05 mg mL^{-1}) was executed by varying the concentrations of Na_2SO_3 (0-0.6 mM) at a fixed K_3[Fe $(CN)_6$] initial concentration of 0.15 mM. Converse assays were carried out at a fixed initial concentration of Na_2SO_3 (0.3 mM) with varied concentrations of K_3[Fe $(CN)_6$] (0-0.2 mM). The initial rate values were adjusted to the Michaelis–Menten model, and the apparent kinetic parameters were calculated based on the Equation: $v_0 = V_{max} \times [S]/ (K_m + [S])$, where v_0 is the initial velocity, V_{max} is the maximal reaction velocity, [S] is the concentration of the substrate and K_m is the Michaelis constant. Mean values of the initial K_3[Fe $(CN)_6$] reduction rates of three traces were used in the calculations.

9. Hot carriers reducing the reaction activation energy through altering the energy of chemical bonds.

The activation energy (E_a) of a reaction is defined as the sum of the activation barrier

for the rate-determining step ($E_{a\text{-}RDS}$)[9]. As previously reported by Caldararu et al[10], the sulfite oxidase (SuOx) reaction might follow the S → OMo mechanism. In the first step, the sulfur atom from the sulfite substrate reacts directly with the equatorial oxo ligand of the Mo ion from SuOx, accompanied with the formation of a Mo-bond sulfate product. Then the product dissociated in the second step. The first step is the rate-determining step (RDS) with a range of barriers (E_{a}-$_{RDS}$). For ML-MoO_x mimetic SuOx reaction, the highest energy barrier is needed for the first transition state (TS1), in which the O_{enzyme} - S_{Sub} bond formed with the reduction of Mo ion (from Mo^{VI} to Mo^{IV}). When excited the surface plasmons of ML-MoO_x, the hot carriers generated and transferred into absorbed sulfite atoms (S_{Sub}) to electronically excite the O_{enzyme} - S_{Sub} bond. Thus, the O_{enzyme} - S_{Sub} bond was activated through an excited state (O_{enzyme} - S_{Sub}*)with a lower activation barrier.

Table S1. Detailed oxygen substoichiometry concentration (x) of molybdenum oxides determined by TGA based on Equation 1.

Sample	x [± 0.003] based on TGA
ML-MoO_x	**1.00**
b-MoO_3	**0.12**

Table S2. Comparison of the kinetic parameters (activation energy, frequency factor) for the SuOx mimetic reaction by ML-MoO_x upon laser on or off.

Light on or off light density (mW cm^{-1})	Activation energy (KJ mol^{-1})	Frequency factor (min^{-1})
—	**83.2**	**2.27×10^{12}**
100	**70.2**	**2.35×10^{10}**
200	**41.9**	**3.56×10^{5}**
300	**38.9**	**1.12×10^{5}**

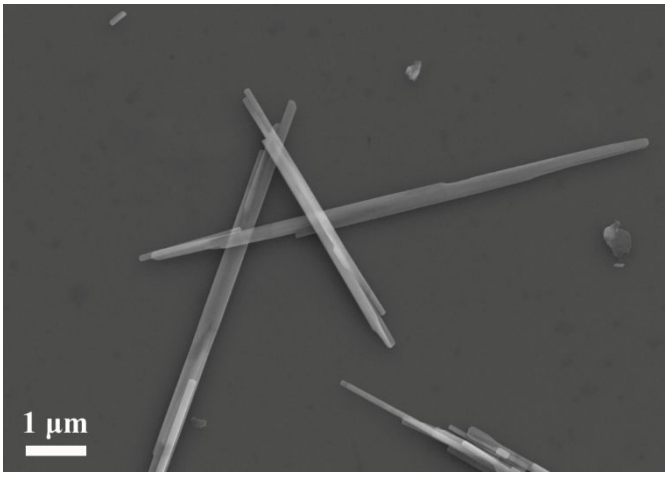

Figure S1. SEM spectra of b-MoO_3.

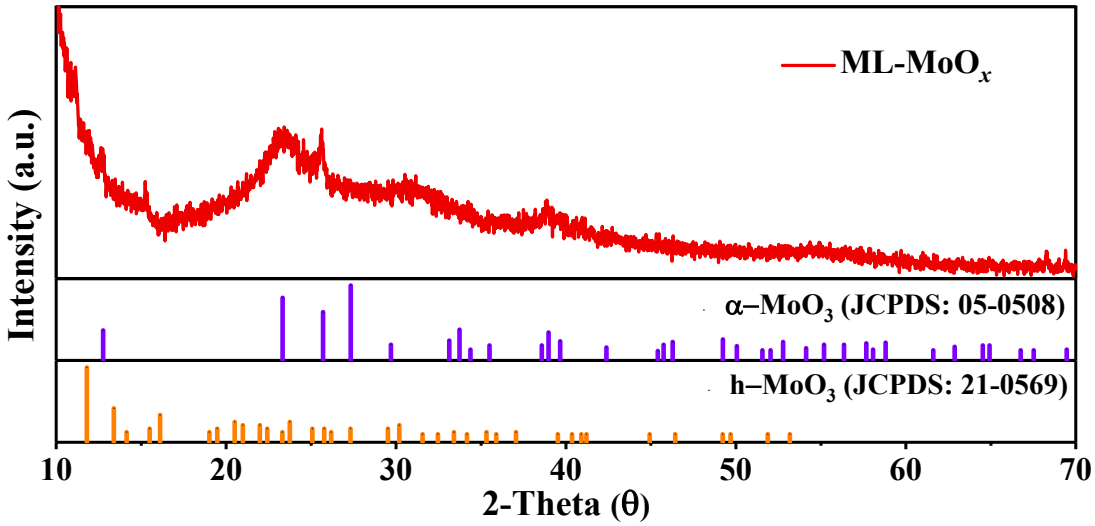

Figure S2. XRD pattern of ML-MoO$_x$.

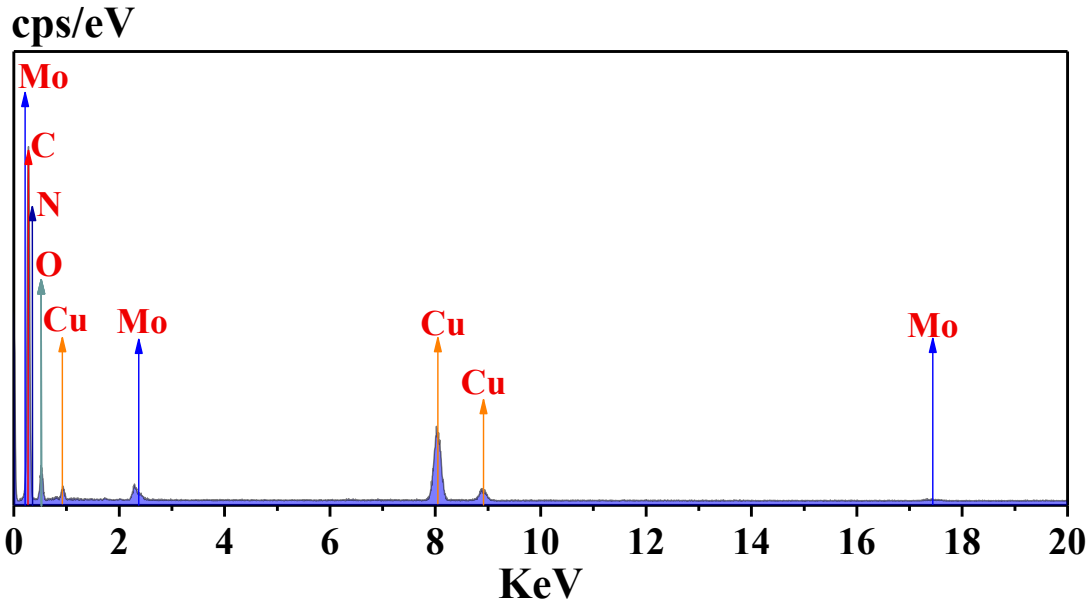

Figure S3. EDS analysis of ML-MoO_x.

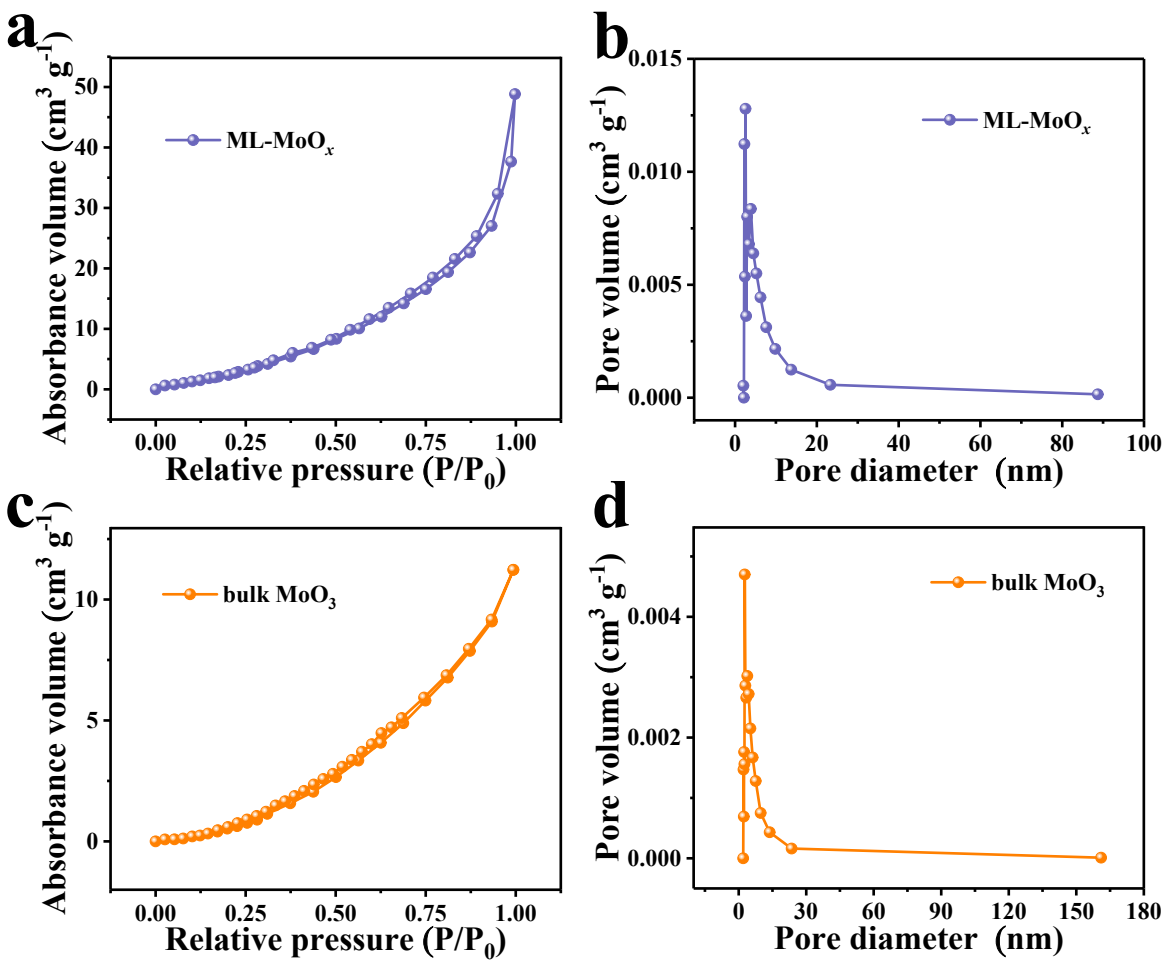

Figure S4. N2 sorption and desorption isotherms of ML-MoO_x (a) and b-MoO_3 (c). (b) and (d) are the corresponding BJH pore size distribution curves.

Figure S5. Optical photos of b-MoO_3 (left) and ML-MoO_x (right).

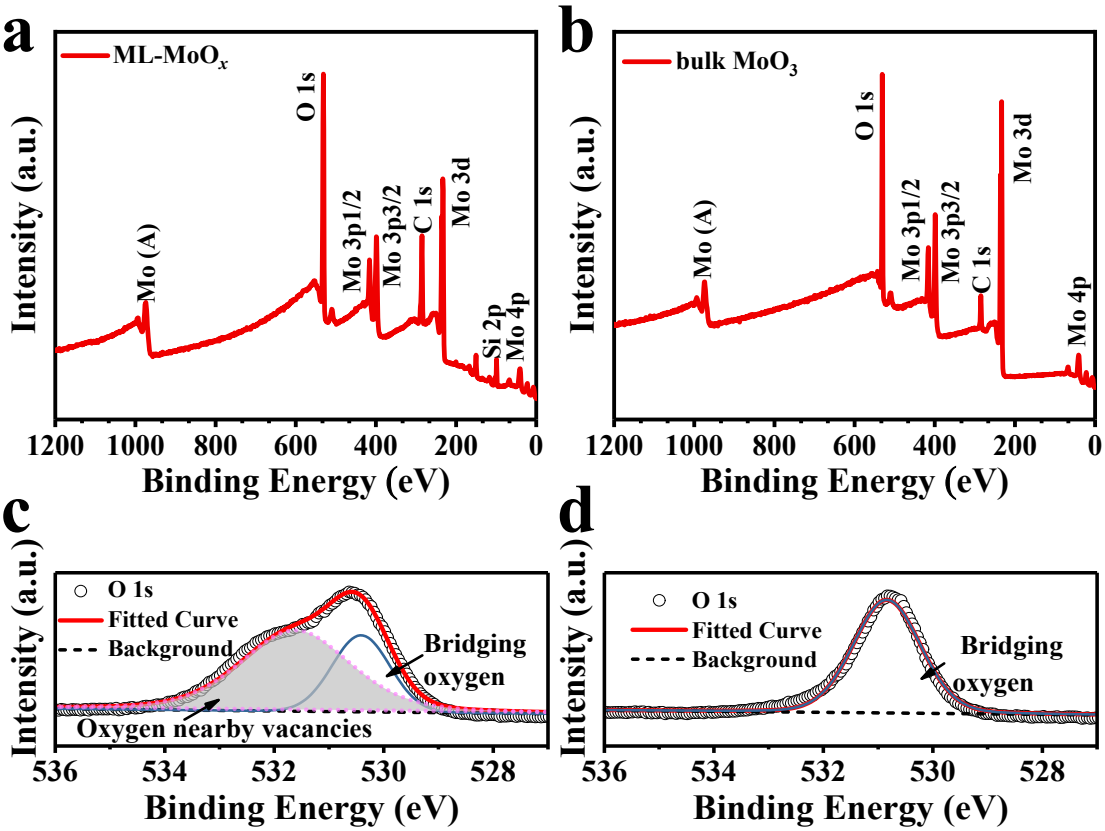

Figure S6. Survey XPS spectra of ML-MoO_x (a) and b-MoO_3 (b). O 1s core level spectra of ML-MoO_x (c) and b-MoO_3 (d).

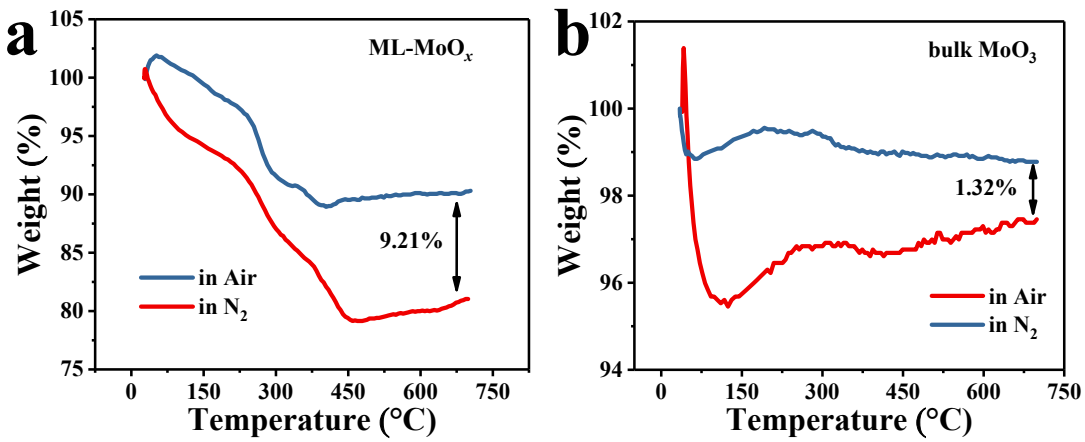

Figure S7. Thermogravimetric analysis (TGA) of ML-MoO_x (a) and b-MoO_3 (b).

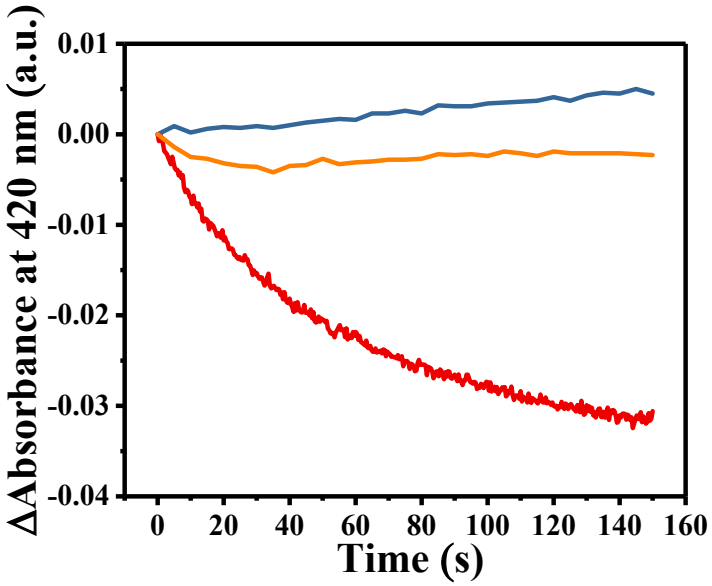

Figure S8. Time-dependent absorbance of $[Fe(CN)_6]^{3-}$ at 420 nm in different reaction systems (ML-MoO_x (0.05 mg mL^{-1}), SO_3^{2-} (0.3 mM) and $[Fe(CN)_6]^{3-}$ (0.15 mM)). (1) ML-MoO_x + SO_3^{2-} + $[Fe(CN)_6]^{3-}$ (red curve), (2) SO_3^{2-} + $[Fe(CN)_6]^{3-}$ (orange curve), (3) ML-MoO_x + $[Fe(CN)_6]^{3-}$.

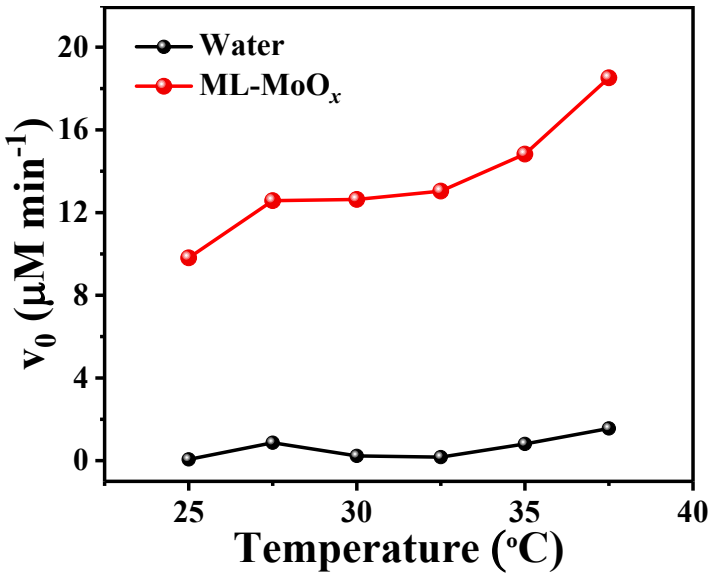

Figure S9. Temperature-dependent study of the control experiments (without the addition of ML-MoO_x) with sulfite (0.3 mM) and $K_3[Fe(CN)_6]$ (0.15 mM). The control SuOx mimetic assays show barely activity, demonstrating that the temperature-dependent catalytic activity is due to intact ML-MoO_x.

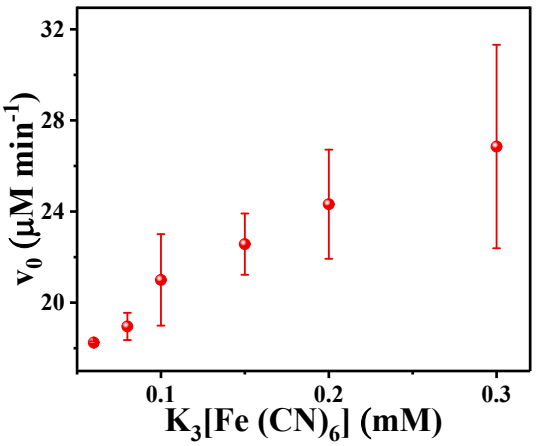

Figure S10. Apparent steady-state kinetic assay of ML-MoO_x at a constant concentration of sulfite (0.3 mM) while varing the concentrations of $[Fe(CN)_6]^{3-}$ from 0 to 0.3 mM (a).

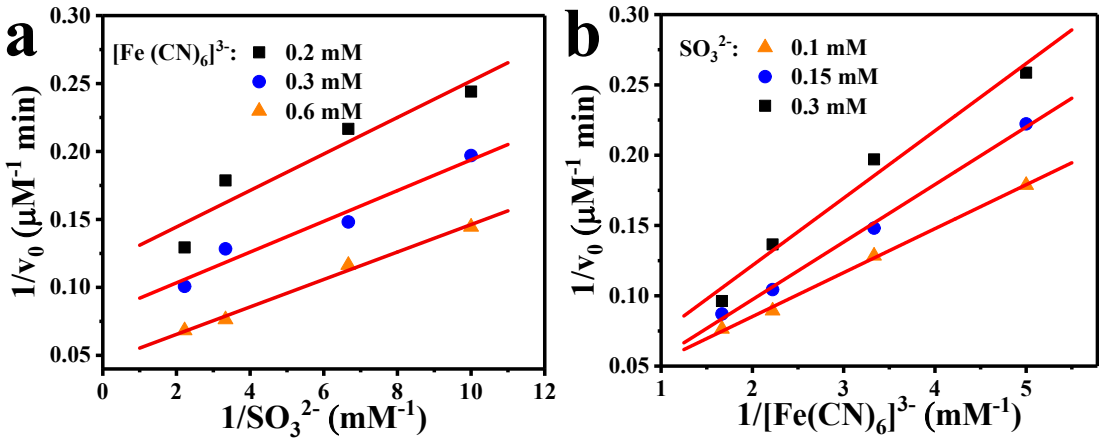

Figure S11. Double-reciprocal plots of ML-MoO_x at a fixed initial concentration of one substrate while varying the concentrations of the other substrate for sulfite and [Fe $(CN)_6]^{3-}$. The error bars represent the standard deviation of three measurements.

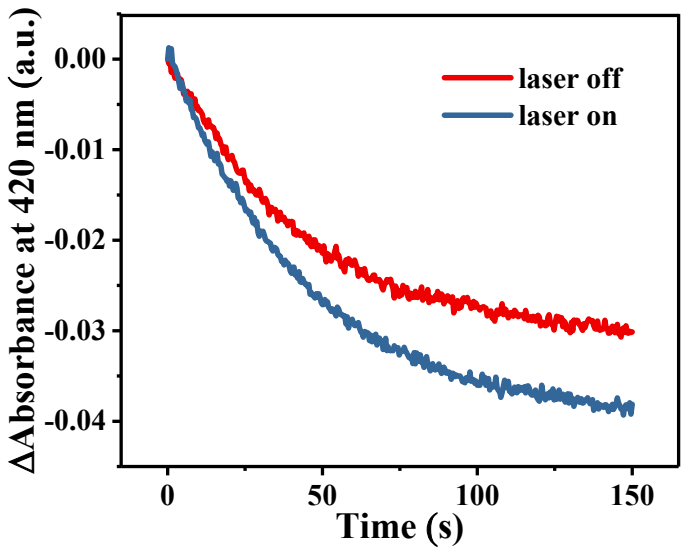

Figure S12. Time-dependent absorbance of $[Fe(CN)_6]^{3-}$ at 420 nm in different upon laser (808 nm, 100 mW cm^{-2}) and off.

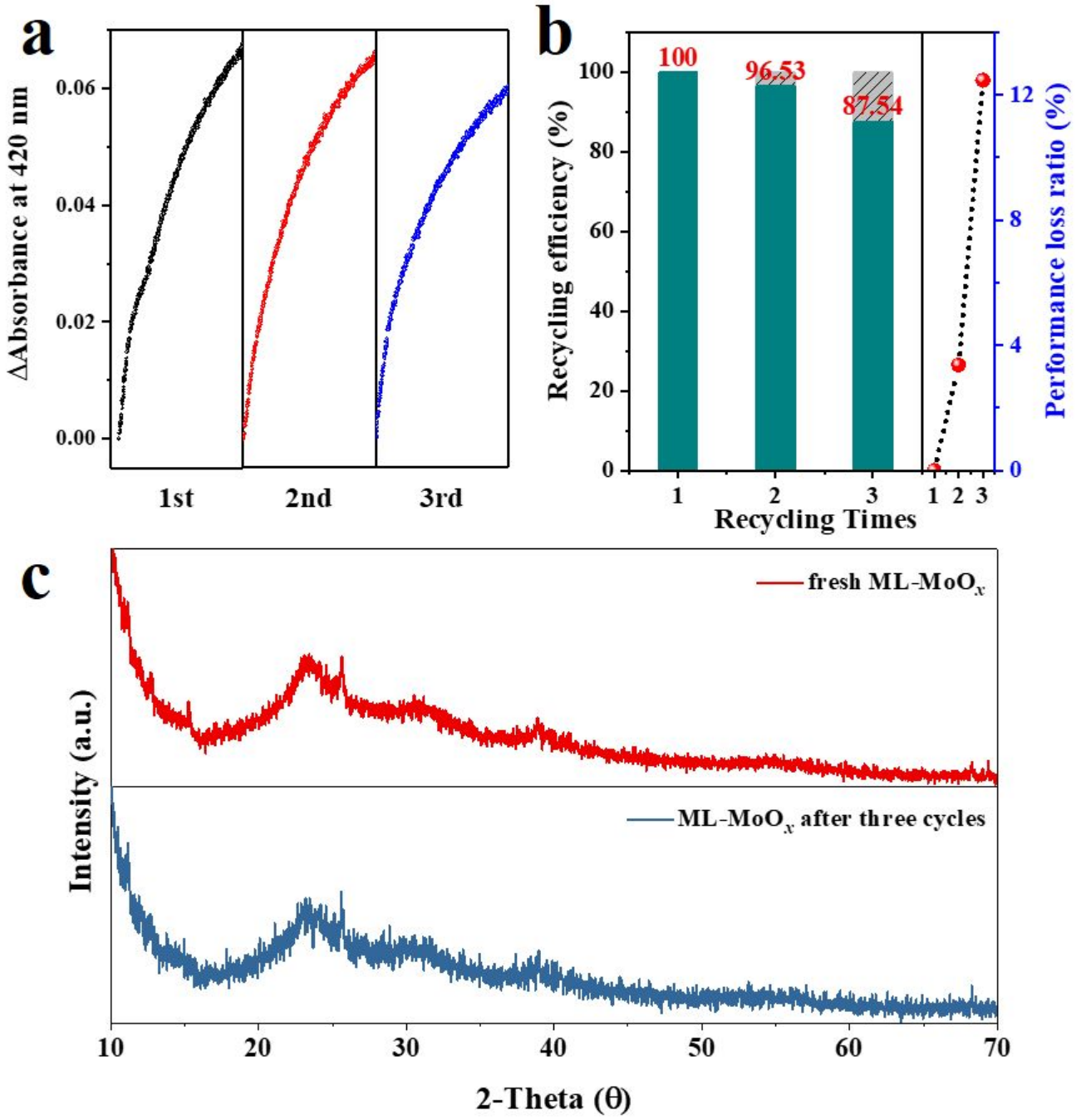

Figure S13. The stability of ML-MoO_x under laser irradiation (808 nm, 300 mW cm^{-1}). (a) Recycling SuOx mimetic tests of ML-MoO_x after three successive cycles. (b) The performance loss in each cycle. (d) XRD patterns of fresh ML-MoO_x and used ML-MoO_x.

S-references

[1] Lu, Q.; Yang, Y.; Feng, J.; Wang, X. Oxygen-Defected Molybdenum Oxides Hierarchical Nanostructure Constructed by Atomic‐Level Thickness Nanosheets as an Efficient Absorber for Solar Steam Generation. *Sol. RRL* **2019,** *3*, 1800277.

[2] Chen, Y.; Chen, T.; Wu, X.; Yang, G. Oxygen Vacancy-Engineered PEGylated MoO_{3-x} Nanoparticles with Superior Sulfite Oxidase Mimetic Activity for Vitamin B1 Detection. *Small* **2019,** *15*, 1903153.

[3] Kim, H. S.; Cook, J. B.; Lin, H.; Ko, J. S.; Tolbert, S. H.; Ozolins, V.; Dunn, B. Oxygen Vacancies Enhance Pseudocapacitive Charge Storage Properties of MoO_{3-x}. *Nat. Mater.* **2017,** *16*, 454-460.

[4] Ragg, R.; Natalio, F.; Tahir, M. N.; Janssen, H.; Kashyap, A.; Strand, D.; Strand, S.; Tremel, W. Molybdenum Trioxide Nanoparticles with Intrinsic Sulfite Oxidase Activity. *Acs Nano* **2014,** *8*, 5182-5189.

[5] Cabre, F.; Cascante, M.; Canela, Ei. A Sensitive Enzymatic Method of Sulfite Determination. *Anal. Lett.* **1990,** *23*, 23-30.

[6] Svitel, J.; Stredansky, M.; Pizzariello, A.; Miertus, S. Composite Biosensor for Sulfite Assay: Use of Water‐Insoluble Hexacyanoferrate(III) Salts as Electron‐Transfer Mediators. *Electroanalysis* **2015,** *10*, 591-596.

[7] Ausaf, A.; Sarfraz, A.; Baig, M. A. Purification and Characterization of Sulfite Oxidase from Goat Liver. *Indian J. Biochem. Bio.* **2008,** *18*, 379-386.

[8] Reisman, M.; Bretschneider, J. C.; Plessen, G. v.; Slimon, U. Reversible Photothermal Melting of DNA in DNA-Gold-Nanoparticle Networks. *Small*. **2008,** *4*,

607-610.

[9] Zhou, L.; Swearer, D. F.; Zhang, C.; Robatjazi, H.; Zhao, H.; Henderson, L.; Dong, L.; Christopher, P.; Carter, E. A.; Nordlander, P. Quantifying Hot Carrier and Thermal Contributions in Plasmonic Photocatalysis. *Science* **2018,** *362*, 69-72.

[10] Caldararu, O.; Feldt, M.; Ciolboc, D.; Van Severen, M. C.; Starke, K.; Mata, R. A.; Nordlander, E.; Ryde, U. QM/MM Study of the Reaction Mechanism of Sulfite Oxidase. *Sci Rep.* **2018,** *8*, 4684.